

Full bandwidth calibration procedure for acoustic probes containing a pressure and particle velocity sensor

Tom G. H. Basten^{a)}

TNO Science and Industry, P.O. Box 155, 2600 AD Delft, The Netherlands

Hans-Elias de Bree

Department of Vehicle Acoustics, HAN University, Ruitenberglaan 26, 6826 CC, Arnhem, The Netherlands

(Received 13 October 2008; revised 6 October 2009; accepted 4 November 2009)

Calibration of acoustic particle velocity sensors is still difficult due to the lack of standardized sensors to compare with. Recently it is shown by Jacobsen and Jaud [J. Acoust. Soc. Am. **120**, 830–837 (2006)] that it is possible to calibrate a sound pressure and particle velocity sensor in free field conditions at higher frequencies. This is done by using the known acoustic impedance at a certain distance of a spherical loudspeaker. When the sound pressure is measured with a calibrated reference microphone, the particle velocity can be calculated from the known impedance and the measured pressure. At lower frequencies, this approach gives unreliable results. The method is now extended to lower frequencies by measuring the acoustic pressure inside the spherical source. At lower frequencies, the sound pressure inside the sphere is proportional to the movement of the loudspeaker membrane. If the movement is known, the particle velocity in front of the loudspeaker can be derived. This low frequency approach is combined with the high frequency approach giving a full bandwidth calibration procedure which can be used in free field conditions using a single calibration setup. The calibration results are compared with results obtained with a standing wave tube. © 2010 Acoustical Society of America. [DOI: 10.1121/1.3268608]

PACS number(s): 43.58.Vb, 43.58.Fm [AJZ]

Pages: 264–270

I. INTRODUCTION

For several years direct measurement of the acoustic particle velocity in air is possible by a particle velocity transducer called the Microflowⁿ.^{1,2} In combination with a small pressure microphone, a very compact pressure-velocity sound probe is available which can be used for direct measurement of impedance,³ sound intensity,⁴ or sound energy.^{5,6} To make proper measurements, one has to know how the output voltage of the sensor relates to the value of the acoustic particle velocity at the measurement location. Also the phase between pressure and velocity sensor has to be accurately known, especially for intensity measurements. Until recently, the calibration of this pressure-velocity probe for the full acoustic bandwidth was quite cumbersome. No reference particle velocity sensor exists, so it is not possible to calibrate a particle velocity sensor by comparing it with a standard reference sensor as is done with microphones. The solution is to create an environment where the acoustic impedance is known. The calibration technique used so far was based on a standing wave tube,^{7,8} which could only be used for low frequencies. Recently a high frequency approach was introduced by Jacobsen and Jaud based on a spherical source.⁹ Although best calibration results were achieved in an anechoic room of good quality, acceptable results were obtained in an ordinary room, which makes this approach very attractive for a standard calibration procedure. However, for low frequencies the approach described by Jacobsen

and Jaud gives unreliable results. Therefore, the method is extended to lower frequencies. In the current paper, a full bandwidth calibration technique for the pressure-velocity sound probe is described. The technique is composed of two parts: one for the lower frequency range and one for the higher frequencies. The results of both calibration steps are combined in the final step. The complete procedure can be performed with a single calibration setup. First, some background of the high and low frequency calibration steps will be given.

II. HIGH FREQUENCY CALIBRATION

For the calibration of a pressure-velocity probe, a special loudspeaker is designed that has a known acoustic impedance,⁹ see Fig. 1. The pressure velocity probe and a reference pressure microphone with a known sensitivity (in the present case a G.R.A.S. 40AC with G.R.A.S. 26AF pre-amplifier is used) will be positioned at certain distance in front of the speaker. The microphone and the pressure-velocity probe are positioned at nearly the same position, see Fig. 1. With the pressure measured with the reference microphone and the known normalized impedance at the measurement location, the pressure-velocity probe can be characterized.

The loudspeaker consists of a hard plastic sphere in which a loudspeaker is placed. This spherical loudspeaker can be modeled as a sphere with radius a and a moving piston with radius b . The relation between sound pressure and particle velocity (the acoustic impedance) on the axis of the piston is given by¹⁰

^{a)}Author to whom correspondence should be addressed. Electronic mail: tom.basten@tno.nl

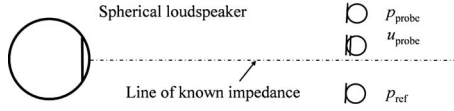


FIG. 1. (Color online) Measurement setup for the piston in a sphere for high frequency calibration.

$$Z_{\text{sphere}}(r) = -j\rho c \frac{\sum_{m=0}^{\infty} (P_{m-1}(\cos \alpha) - P_{m+1}(\cos \alpha)) \frac{h_m(kr)}{h'_m(ka)}}{\sum_{m=0}^{\infty} (P_{m-1}(\cos \alpha) - P_{m+1}(\cos \alpha)) \frac{h'_m(kr)}{h'_m(ka)}}, \quad (1)$$

where r is the distance from the centre of the sphere, $\alpha = \arcsin(b/a)$, a is the radius of the sphere, b is the radius of the loudspeaker, P_m is the Legendre function of the order m , h_m is the spherical Hankel function of the second kind and order m , h'_m is its derivative, ρ is the density of the air, and c is the speed of sound in air. The calibration results are normalized with the specific impedance ρc . The sensitivity of the particle velocity sensor will therefore be given in mV/Pa^* , where 1 Pa^* corresponds to $1 \text{ Pa}/\rho c \approx 2.4 \text{ mm/s}$. The specific impedance depends on environmental conditions, such as temperature, atmospheric pressure, and relative humidity.

Although the (normalized) impedance on the axis of the spherical source is described by the complex expression (1), the resulting impedance is quite similar to the acoustic impedance at a certain distance r of a monopole source, given by

$$Z(r) = \rho c \frac{jkr}{1 + jkr}. \quad (2)$$

The ratio of the impedance of the piston (diameter piston 6.5 cm) in a sphere (diameter 20.5 cm), described by Eq. (1) and the acoustic impedance of a monopole source [Eq. (2)], is given in Fig. 2 for varying distance from the front of the sphere. As can be expected, the difference between both impedance descriptions is largest at a short distance from the source and for low frequencies.

For the calibration procedure in the current paper, the standard pressure-velocity probe is used. This probe has a 0.5 in. packaging for protection and increases the sensitivity of the particle velocity sensor. However, this packaging means that the PU probe can be used under 10 kHz. Above these frequencies, the packaging has too much influence on the measured sound field.

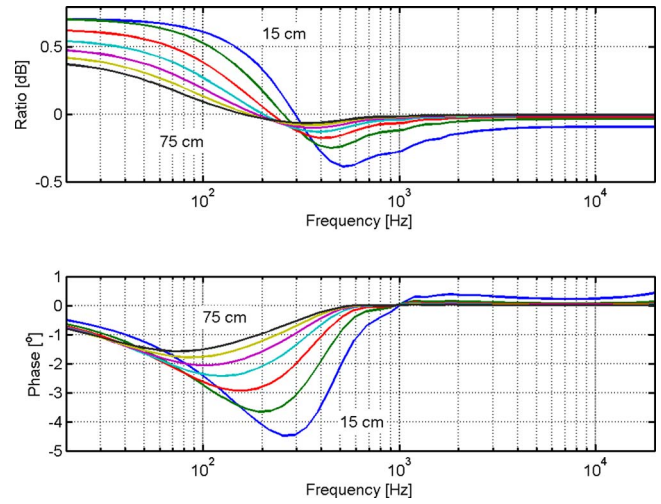


FIG. 2. (Color online) The ratio between the impedance at a certain distance in front of a piston in a sphere and the impedance in front of a monopole (diameter piston 6.5 cm, diameter sphere 20.5 cm). The distance from the front of the sphere is increased from 15 to 75 cm in steps of 10 cm. The dB scale in the upper figure is defined by $20 \log$ (amplitude ratio).

III. LOW FREQUENCY CALIBRATION

At lower frequencies, the calibration procedure described in Sec. II has some drawbacks. In an ordinary room, at lower frequencies the background noise has higher pressure levels than the noise that is generated by the source. This is shown in Fig. 3 where some measurement results are given. The output of the microphone with the source on and the output when the source is switched off are given in the upper figure (all measurements are done with a Siglab 20–42 signal analyzer with a frequency resolution of 1.5625 Hz). As can be seen, the background noise is dominant for frequencies below 50 Hz. For the particle velocity, this effect is not observed, see the lower figure. There, the difference between background noise and the emitted signal from the loudspeaker is much higher. The main reason for this observation is that in the near field of a sound source the ratio between particle velocity and pressure increases. For a monopole this can be easily observed by applying Eq. (2). So

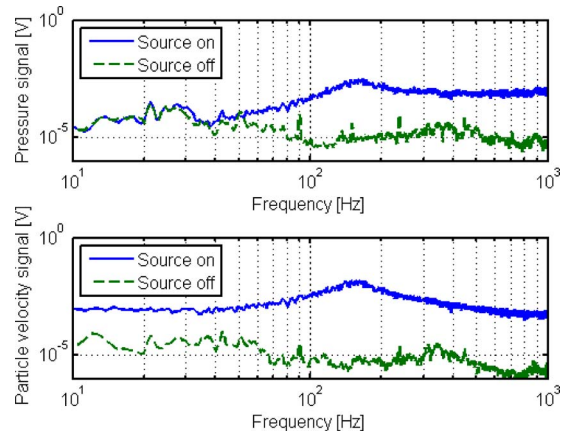


FIG. 3. (Color online) Pressure and velocity signals just in front of the moving piston with source switched on and off. At low frequencies, the microphone signal is clearly more affected by background noise than the particle velocity signal.

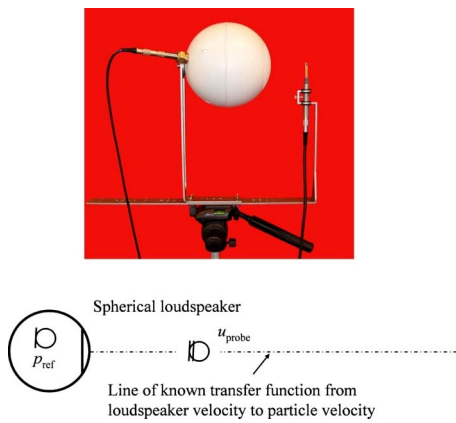


FIG. 4. (Color online) Measurement setup for the low frequency calibration. The pressure microphone is now put inside the spherical loudspeaker.

for low frequencies, when the probe is in the near field of the source, the ratio between particle velocity and acoustic pressure is significant. For the background noise, for which the probe is in the far field, the ratio between pressure and particle velocity is similar as for high frequencies.

Therefore, in an anechoic room with low background noise, the method described in Sec. II will work down to 50 Hz.⁹ In an ordinary room, the background noise is higher and the method starts to work properly from 100 to 200 Hz. The sound pressure microphone, however, can be calibrated in the frequency range 20–10 kHz, because its calibration is based on the comparison with the output of the reference microphone which is at the same position. Both sensors are omnidirectional and it is of no consequence if the output is caused by background noise or by the spherical loudspeaker. For the particle velocity sensor, this does not hold because its calibration is based on the known impedance due to the loudspeaker. When the background noise becomes dominant, Eq. (1) cannot be applied anymore. Therefore, depending on the amount of background noise, the velocity sensor can be calibrated in the frequency range from several hundreds of Hertz to about 10 kHz. For the low frequencies, a different approach will be followed, see Fig. 4.

Now the reference microphone is put into a hole in the sphere and tightened with rubber rings. The reference microphone measures the interior pressure variations in the sphere and the relation between the interior pressure and the particle velocity at a distance in front of the sphere will be used for calibration. The advantage is that the pressure inside the sphere is sufficiently high down to lower frequencies and there is a simple relation between the interior pressure and the particle velocity at the probe position. For low frequencies (well below the first internal acoustic resonance of the sphere), the frequency response between the interior pressure and velocity of the membrane of the loudspeaker is inversely proportional to the frequency. Due to the continuity condition, the particle velocity just in front of the membrane is similar to the velocity of the membrane itself. Therefore, the relation between the sound pressure in the sphere and the particle velocity u_n just in front of the membrane is given by

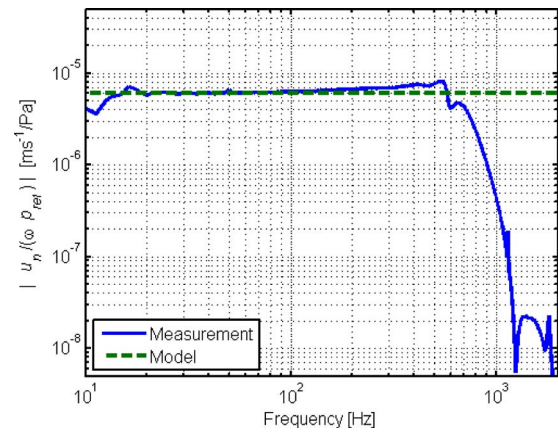


FIG. 5. (Color online) Transfer function between pressure in the sphere and the displacement of the membrane. The displacement is calculated by $|u_n/\omega|$.

$$u_n = -\frac{j\omega V_0}{\gamma A_0 p_0} p_{\text{ref}} \quad (3)$$

where ω is the angular frequency, V_0 is the interior volume of the sphere, A_0 is the surface area of the moving piston, p_0 is the ambient pressure, and γ is the ratio of specific heats (1.4 for normal air). It is assumed that the compression and rarefaction of the air in the sphere is an adiabatic process.

To verify that this relation is valid, a simple experiment is performed, see Fig. 5. Here the transfer function between the sound pressure in the sphere and the displacement of the membrane is given. The displacement is measured by integrating twice the output of an accelerometer, which for this measurement is glued on the membrane of the loudspeaker. According to Eq. (3), the transfer function between pressure and displacement is frequency independent. In Fig. 5, it is clear that this independency is found from 10 Hz up to about 300 Hz. In this figure also the theoretical model is given, where it is assumed that the internal volume of the sphere is $2.8 \times 10^{-3} \text{ m}^3$ (corresponding to 17.5 cm internal diameter) and that the surface area is $3.3 \times 10^{-3} \text{ m}^2$ (corresponding to a piston with diameter of 6.5 cm).

For higher frequencies, the method fails because of internal acoustic modes in the sphere. If the wavelength is smaller than the dimensions of the sphere, the sound pressure is not uniform in the sphere and the simple relation given by Eq. (3) is not valid anymore.

Because the characteristics of an acoustic field around a sphere with a moving piston are known, also the particle velocity at a certain distance in front of the moving piston can be derived when the particle velocity just in front of the piston is known. Therefore, the particle velocity at the measurement position can be related to the interior pressure of the sphere.

The relation between the particle velocity just in front of the piston, which equals the normal velocity of this piston (u_n) and the particle velocity at a distance r from the centre of the sphere, is given by¹⁰

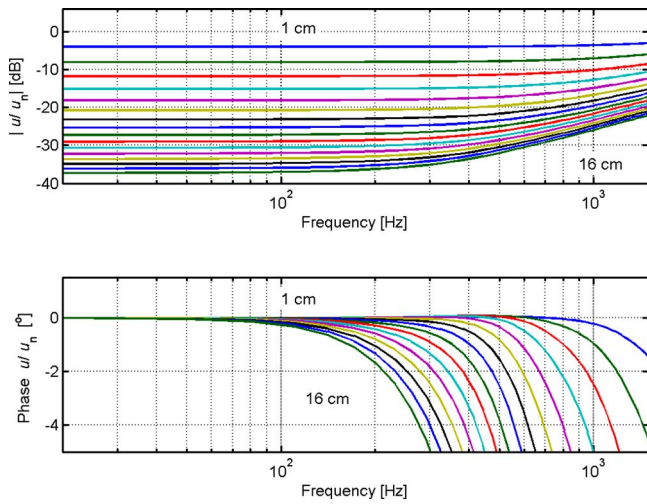


FIG. 6. (Color online) Transfer function between particle velocities at several distances from the moving piston and the particle velocity just in front of the piston as given by Eq. (4). The diameter of the sphere is 20.5 cm and the piston diameter is 6.5 cm. The dB scale in the upper figure is defined by 20 log (amplitude ratio).

$$u(r) = -\frac{u_n}{2} \sum_{m=0}^{\infty} (P_{m-1}(\cos \alpha) - P_{m+1}(\cos \alpha)) \frac{h'_m(kr)}{h'_m(ka)}. \quad (4)$$

The ratio of the surface velocity of the loudspeaker (u_n) to the particle velocity $u(r)$ measured from 1–16 cm in front of a piston (6.5 cm) in a sphere (20.5 cm) calculated with Eq. (4) is given in Fig. 6. It is clear that for lower frequencies (< 200 Hz), the amplitude is almost independent of the frequency and the phase difference is almost zero. This means that the phase difference between the reference pressure microphone in the sphere and the particle velocity sensor has to be 90° [see Eq. (3)]. This fact can be used for calibration.

As a check for this behavior, a measurement is performed. The transfer function is measured between the particle velocity 1 cm in front of the piston and the particle velocity at 14 cm, see Fig. 7. As can be clearly seen, the phase difference at low frequencies (< 200 Hz) is almost

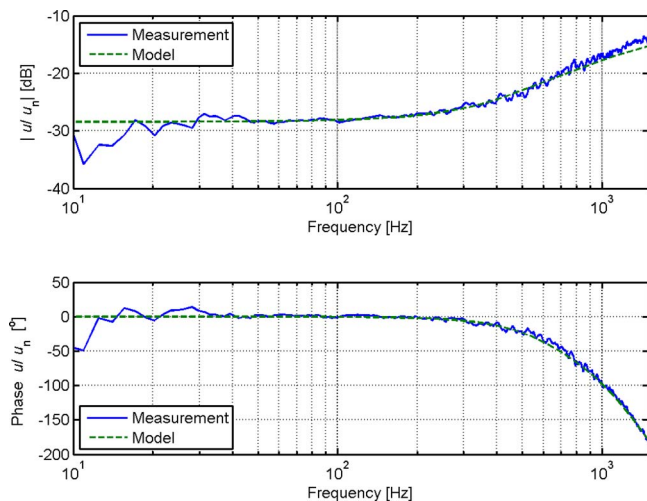


FIG. 7. (Color online) Measured and modeled transfer functions of particle velocities measured at 1 cm and at 14 cm in front of the large spherical loudspeaker. (Upper) Modulus. (Lower) Phase.

zero, as is also predicted by the model, for which the results are also plotted in this figure. The measurement results are in very good agreement with the model.

Combining Eqs. (3) and (4) gives a relation between the particle velocity at position r and the pressure in the piston. This means that when the interior acoustic pressure of the sphere is measured, the (normalized) particle velocity at distance r is exactly known. This known particle velocity value is used for calibration. This can only be done for frequencies, well below the first internal resonance frequency of the sphere. For higher frequencies, the pressure inside the sphere is not uniform anymore. With a correction, taking into account the effect of the first internal resonance frequency of the sphere, the low frequency approach can be applied up to higher frequencies.

IV. COMBINING THE LOW AND HIGH FREQUENCY APPROACHES

Two steps to determine the full bandwidth sensitivity and phase characteristics of the pressure-velocity probe are described, one for the high frequency range and one for the low frequency range. These two results are combined in the final step. It will be shown that the high frequency approach and low frequency approach give similar results in the medium frequency range around 300 Hz.

The complete procedure is now as follows. First, a measurement is performed with the high frequency configuration. That means that the reference pressure sensor and the pressure-velocity probe are placed at a known position on the axis of the spherical source, while white noise is emitted. The transfer functions between all sensors are measured. The ratio of the reference microphone output (in volts) and the output of the pressure sensor (in volts) is directly used to determine the sensitivity S_p (mV/Pa) of the pressure sensor:

$$S_p \left[\frac{\text{mV}}{\text{Pa}} \right] = \frac{p}{p_{\text{ref}}} \left[\frac{\text{V}}{\text{V}} \right] \cdot S_{\text{ref}} \left[\frac{\text{mV}}{\text{Pa}} \right], \quad (5)$$

where S_{ref} is the known sensitivity of the reference microphone (14 mV/Pa), which is assumed to be independent of frequency in the frequency range of interest and independent of the static pressure.

The particle velocity cannot directly related to the reference sensor output. Here the model of the impedance of the piston in a sphere, Eq. (1), has to be used. The sensitivity of the particle velocity sensor S_u [mV/Pa*] is calculated by

$$S_u \left[\frac{\text{mV}}{\text{Pa}^*} \right] = \frac{u}{p_{\text{ref}}} \left[\frac{\text{V}}{\text{V}} \right] \cdot Z_{\text{sphere}} \left[\frac{\text{Pa}}{\text{Pa}^*} \right] \cdot S_{\text{ref}} \left[\frac{\text{mV}}{\text{Pa}} \right]. \quad (6)$$

Now the sensitivity of the pressure sensor of the probe is known for the complete frequency range and the sensitivity of the particle velocity sensor only for the high frequency range.

Next, the reference pressure sensor is put in the hole of sphere and tightened with rubber rings so that the sphere is leakage-free. The pressure-velocity probe is placed at a known position in front of the moving membrane, but closer than in the previous step (about 1 cm in front of the moving

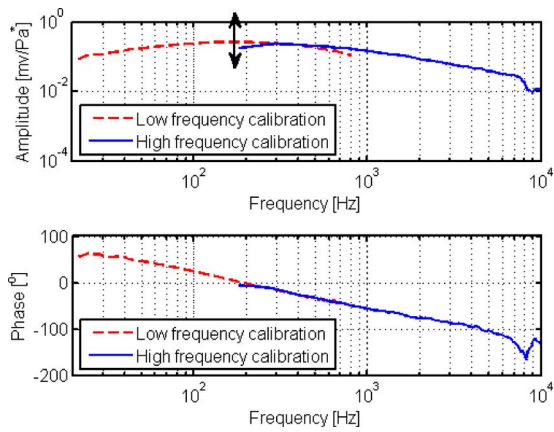


FIG. 8. (Color online) Low and high frequency calibrations, combined.

piston). Again all transfer functions are measured while white noise is emitted by the source. The particle velocity is now calculated based on Eqs. (3) and (4):

$$S_u \left[\frac{\text{mV}}{\text{Pa}^*} \right] = \frac{u}{p_{\text{ref}}} \left[\frac{\text{V}}{\text{V}} \right] \cdot \frac{u_n}{u} \left[\frac{\text{Pa}^*}{\text{Pa}^*} \right] \cdot \frac{p_{\text{ref}}}{u_n} \left[\frac{\text{Pa}}{\text{Pa}^*} \right] \cdot S_{\text{ref}} \left[\frac{\text{mV}}{\text{Pa}} \right]. \quad (7)$$

In the next step, the low and high frequency curves are connected. For the amplitude, see Fig. 8, upper, the low frequency calibration curve (< 350 Hz) is tuned such that it connects with the high frequency curve. The parameters in Eq. (7) to make this connection are $\rho = 1.2 \text{ kg/m}^3$, $c = 340 \text{ m/s}$, $V_0 = 2.8 \times 10^{-3} \text{ m}^3$ and $A_0 = 3.3 \times 10^{-3} \text{ m}^2$. The phase is continuous over the frequency. For the low frequency approach around 350 Hz, the phase is exactly known. For the high frequency part, a discontinuity can be introduced by the correction term [Eq. (1)]. Within this term, the distance between the probe and the source is the most important parameter which can be used to tune the phase, such that it connects with the low frequency part. The low and high frequency calibration curves have a small overlap around 350 Hz. Around this frequency, both curves can be combined to create a full bandwidth calibration curve.

Before connecting the low and high frequency calibration curves, the complex sensitivities for the high frequency approach are smoothed. Because of the reflections in the ordinary room, the determined sensitivities seem rather noisy. This is avoided by smoothing the results by a moving average filter.¹¹ Another technique to smooth the curves is a time selective technique. In this way room reflections can be removed by canceling the reflected signals in the impulse response. However, this method is not very accurate for low frequencies.¹²

V. COMPARISON WITH STANDING WAVE TUBE CALIBRATION

Another environment where the acoustic impedance is exactly known is in the interior of a rigidly terminated tube where a sound wave is generated by a speaker,⁸ see Fig. 9 and schematically in Fig. 10.

This tube is also known as the standing wave tube and can be used as an alternative for calibration at low frequen-

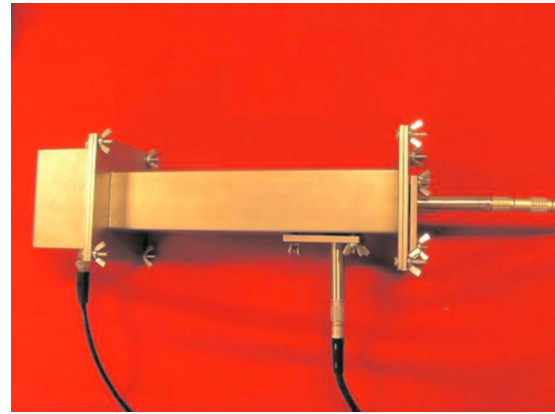


FIG. 9. (Color online) Small standing wave tube for low frequency calibration of the pressure-velocity probe.

cies. With the reference pressure sensor at the rigid end of the tube, the pressure and particle velocity are known at each location in the tube. This tube can therefore be used for calibration of the particle velocity sensor. However, it only works down to low frequencies below the cut-off frequency f_c of the tube, which is determined by the diameter of the tube d and the speed of sound:

$$f_c = \frac{c}{1.71d}. \quad (8)$$

Above the cut-off frequency (which is about 4.5 kHz for the current tube), the sound field is not one-dimensional anymore, i.e., the sound pressure across the cross section of the tube is not uniform and the impedance cannot be described anymore with simple relations. Non-ideal behavior, such as damping due to viscous and thermal effects and non-ideal reflection of the rigid termination, can be neglected.⁸

The relation between pressure $p(x)$ and particle velocity $u(x)$ at an arbitrary location in the tube is given by

$$\frac{u(x)}{p(x)} = \frac{j}{\rho c} \tan(k(l-x)). \quad (9)$$

The sensitivity of the pressure microphone S_p and the particle velocity S_u of the probe can be calculated by

$$S_p \left[\frac{\text{mV}}{\text{Pa}} \right] = \frac{p}{p_{\text{ref}}} \left[\frac{\text{V}}{\text{V}} \right] \frac{1}{\cos(k(l-x))} S_{\text{ref}} \left[\frac{\text{mV}}{\text{Pa}} \right], \quad (10)$$

$$S_u \left[\frac{\text{mV}}{\text{Pa}^*} \right] = \frac{u}{p_{\text{ref}}} \left[\frac{\text{V}}{\text{V}} \right] \frac{1}{j \sin(k(l-x))} S_{\text{ref}} \left[\frac{\text{mV}}{\text{Pa}} \right]. \quad (11)$$

A short standing wave tube as given in Fig. 9 is used for calibration for low frequencies. The inner dimensions of the tube are $47 \times 47 \text{ mm}^2$ and the probe is positioned such that $l-x = 55 \text{ mm}$. While white noise is emitted by the loudspeaker, the transfer functions p/p_{ref} and u/p_{ref} are measured. The sensitivities are calculated by Eqs. (10) and (11),

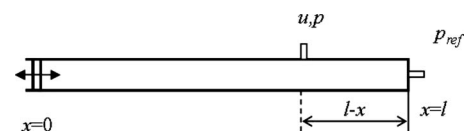


FIG. 10. Schematic representation of the standing wave tube.

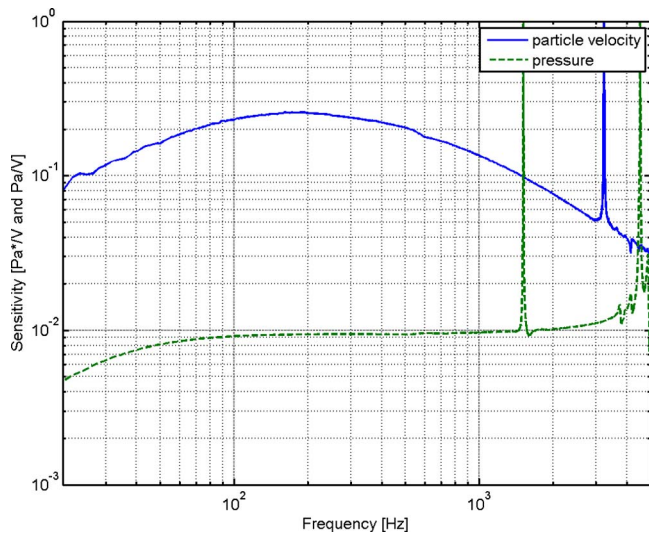


FIG. 11. (Color online) Calculated sensitivities of the particle velocity sensor and the pressure sensor.

where the reference microphone has a sensitivity of 14 mV/Pa. The calculated sensitivities are given in Fig. 11.

The calculated phase response of the pressure and particle velocity sensor relative to the reference pressure sensor is given in Fig. 12.

The calibration results of the particle velocity sensor measured with the sphere setup and standing wave tube setup are compared in Fig. 13. Both the absolute amplitude and phase responses are given. In Fig. 14, the difference between the standing waving tube and the sphere calibration for low frequencies is given. Up to 400 Hz, the error in magnitude is less than 0.5 dB and the phase error is smaller than 4°. The deviations are probably caused by experimental inaccuracies. Especially the offset in the phase error is probably caused by a small leakage during the standing wave tube experiments.

VI. DISCUSSION

The results given in the current paper are all obtained in an ordinary room with background noise due to all kind of

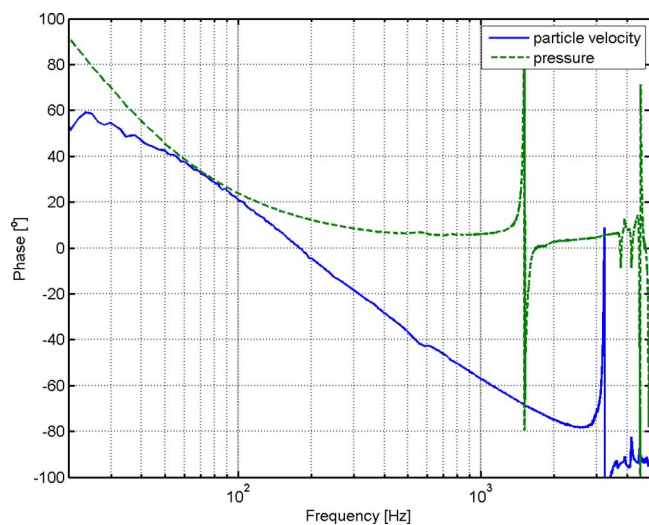


FIG. 12. (Color online) Phase response of particle velocity and pressure sensors of the pressure-velocity probe relative to the reference pressure sensor.

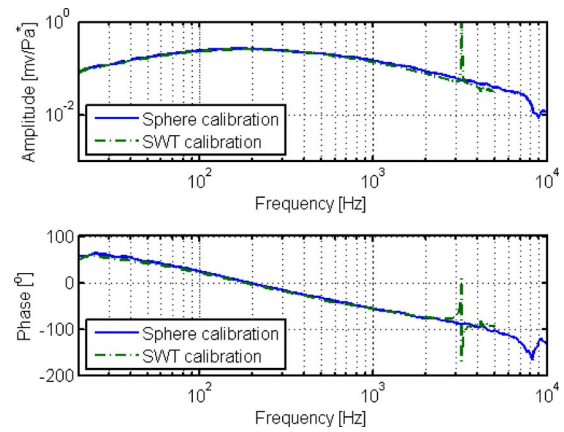


FIG. 13. (Color online) Results of calibration of the particle velocity probe. The curves for the sphere calibration, and the standing wave tube results are given. (Upper) Amplitude. (Lower) Phase.

activities in the neighborhood. Because the measurements are performed very close or even inside the sphere, the calibration results seem to be still very good. The influence of reflections due to the floor, wall, and furniture inside the room are canceled by smoothing the results with a moving average filter. There is a good indication that the proposed method is valid both for low and high frequencies. The comparison with a standing wave tube shows the accuracy for low frequencies and in the paper by Jacobsen and Jaud,⁹ the accuracy for higher frequencies is demonstrated. However, because there are many potential errors, a complete sensitivity study for the different parameters involved should be performed. In the paper by Jacobsen and Jaud,⁹ it is, for instance, shown that the distance between the probe and the sphere has no significant influence and the calibration performed at several source probe distances agreed within ± 0.3 dB and $\pm 1^\circ$ above 100 Hz. However, the exact distance between probe and source is difficult to determine, but can be found because the phase relation for low frequencies is accurately known. Using this fact, the distance between probe and source can be used as the parameter to tune the phase for high frequencies such that it fits to the low fre-

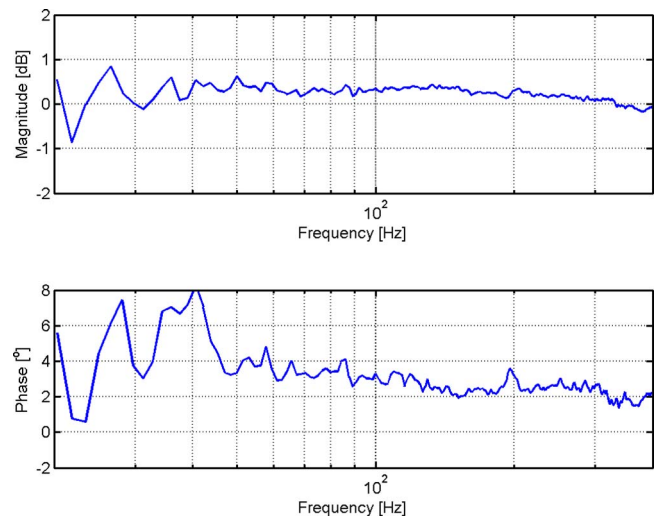


FIG. 14. (Color online) Difference between standing wave calibration and the sphere calibration.

quency phase. Therefore, the combination of high and low frequency results make the approach described in this paper very strong.

VII. CONCLUSIONS

A full bandwidth calibration procedure for pressure-velocity probes is described, based on the known sound field around a spherical source, which is modeled as a sphere with a moving piston. For lower frequencies (< 1 kHz), the velocity sensor of the probe is calibrated close in front of the spherical loudspeaker and the reference sound pressure microphone is measuring the interior sound pressure of the sphere which is directly related to the piston motion. For higher frequencies (> 100 Hz) the pressure-velocity probe is calibrated in front of a spherical loudspeaker in combination with a reference sound pressure microphone. Room reflections are canceled by a moving average technique in the frequency domain. Low and high frequency results, obtained with the same calibration setup, are combined at intermediate frequencies yielding the amplitude and phase response of the pressure velocity probe in the full acoustic bandwidth.

ACKNOWLEDGMENTS

This research is financially supported by the Netherlands Organization for Scientific Research NWO within the Casimir program (stimulating knowledge exchange between research institutes and industry).

¹H. E. de Bree, "The Microflown, an acoustic particle velocity sensor," *Acoust. Aust.* **31**, 91–94 (2003).

²H. E. de Bree, "An overview of Microflown Technologies," *Acta. Acust. Acust.* **89**, 163–172 (2003).

³R. Lanoye, G. Vermeir, W. Lauriks, R. Kruse, and V. Mellert, "Measuring the free field acoustic impedance and absorption coefficient of sound absorbing materials with a combined particle velocity-pressure sensor," *J. Acoust. Soc. Am.* **119**, 2826–2831 (2006).

⁴F. Jacobsen and H.-E. de Bree, "A comparison of two different sound intensity measurement principles," *J. Acoust. Soc. Am.* **118**, 1510–1517 (2005).

⁵D. B. Nutter, T. W. Leishman, S. D. Sommerfeld, and J. D. Blotter, "Measurement of sound power and absorption in reverberation chambers using energy density," *J. Acoust. Soc. Am.* **121**, 2700–2710 (2007).

⁶F. Jacobsen, "Measurement of total sound energy density in enclosures at low frequencies," in *Acoustics08*, Paris, France (2008).

⁷D. Stanzial and D. Bonsi, "Calibration of the p-v Microflown[®] probe and some considerations on the physical nature of sound impedance," in *Euronoise*, Naples, Italy (2003).

⁸R. Raangs, T. Schlicke, and R. Barham, "Calibration of a micromachined particle velocity microphone in a standing wave tube using a LDA photon-correlation technique," *Meas. Sci. Technol.* **16**, 1099–1108 (2005).

⁹F. Jacobsen and V. Jaud, "A note on the calibration of pressure velocity sound intensity probes," *J. Acoust. Soc. Am.* **120**, 830–837 (2006).

¹⁰E. G. Williams, *Fourier Acoustics: Sound Radiation and Nearfield Acoustical Holography* (Academic, New York, 1999).

¹¹H. E. de Bree, M. Nosko, and E. Tijs, "A handheld device to measure the acoustic absorption in situ," in *Fifth International Styrian Noise, Vibration and Harshness Congress*, Graz, Austria (2008).

¹²H. E. de Bree, R. Lanoye, S. de Cock, and J. van Heck, "In situ, broad band method to determine the normal and oblique reflection coefficient of acoustic materials," in *SAE Noise and Vibration Conference and Exhibition*, Grand Traverse, MI (2005), SAE Technical Paper No. 2005-01-2443.